Soft Matter

PAPER

View Article Online
View Journal | View Issue

Cite this: *Soft Matter*, 2015, **11**, 5030

Celebrating *Soft Matter*'s 10th anniversary: screening of the calcium-induced spontaneous curvature of lipid membranes

Mijo Simunovic,[ab] Ka Yee C. Lee[b] and Patricia Bassereau*[a]

Received 14th January 2015,
Accepted 11th May 2015

DOI: 10.1039/c5sm00104h

www.rsc.org/softmatter

Lipid membranes are key regulators of cellular function. An important step in membrane-related phenomena is the reshaping of the lipid bilayer, often induced by binding of macromolecules. Numerous experimental and simulation efforts have revealed that calcium, a ubiquitous cellular messenger, has a strong impact on the phase behavior, structural properties, and the stability of membranes. Yet, it is still unknown the way calcium and lipid interactions affect their macroscopic mechanical properties. In this work, we studied the interaction of calcium ions with membrane tethers pulled from giant unilamellar vesicles, to quantify the mechanical effect on the membrane. We found that calcium imposes a positive spontaneous curvature on negatively charged membranes, contrary to predictions we made based on the proposed atomic structure. Surprisingly, this effect vanishes in the presence of physiologically relevant concentrations of sodium chloride. Our work implies that calcium may be a trigger for membrane reshaping only at high concentrations, in a process that is robustly screened by sodium ions.

Introduction

The calcium ion is a major signaling species that takes part in numerous cellular processes.[1] It significantly alters the local electrostatics of macromolecules and, by doing so, it can trigger a conformational change in some proteins.[2,3] Being a powerful cellular messenger, its equilibrium cytosolic concentration is kept at $\sim$100 nM, four orders of magnitude lower than that outside the cell.[1] Calcium also interacts with lipid membranes, which may drive large-scale morphological transformations, such as membrane fusion.[4]

The effect of calcium on lipid membranes has been studied for decades. Early on, it was shown that calcium couples with the phase behavior, structural properties, and the stability of bilayers.[5–7] More recently, tremendous experimental and simulation efforts have been made to elucidate the interactions of calcium with lipid bilayers, in light of significantly varying views on the precise atomic aspects of this phenomenon.[8,9] This variation is often attributed to the measuring methodology or experimental conditions, such as the concentration of calcium or other ions.[8]

Studies on monolayers composed of phosphatidylinositol 4,5-bisphosphate (PIP_2) revealed that ions have a marked effect on the organization of lipids. Specifically, monovalent cations induce the expansion of PIP_2 monolayers, while divalent cations compress them.[10] The same authors did not observe an appreciable effect of Na^+ on phosphatidylserine (PS) monolayers, although others have reported a reduction of the lipid area upon Ca^{2+} binding to PS-containing bilayers.[9,11] Simulations have shown that Na^+ penetrates deep into the bilayer.[12–14] Calcium ions, on the other hand, seem to be coordinated at the level of the phosphate group in both PS and PIP_2 membranes.[15,16] This structural arrangement and the reported dehydration of the bilayer upon calcium binding[8,17] most likely result in the tighter packing of lipids leading to a reduction in the lipid area.

Binding of calcium may even drive the formation of heterogeneities in the lateral composition of the membrane. In particular, studies have shown calcium-induced clustering of PIP_2 in monolayers and bilayers composed of phosphatidylcholine (PC) and PIP_2.[10,16] Moreover, calcium causes demixing of PS-containing monolayers at lower lateral pressure.[11]

In light of the numerous effects calcium can impart on the membrane, it is expected that its binding leads to macroscopic changes in the structure of the bilayer. However, it is still unclear whether Ca^{2+} affects the mechanical and morphological properties of the membrane, such as bending rigidity or the spontaneous curvature. Cell membranes in great part comprise PC and PS lipids, especially in the cytosolic leaflet,[18] therefore it is of key importance to understand all aspects of how this ubiquitous signaling ion interacts with PS-containing membranes. Our aim in this work is to investigate and quantify

[a] *Institut Curie, Centre National de la Recherche Scientifique, Unité Mixte de Recherche 168, Université Pierre et Marie Curie, F-75248 Paris, France. E-mail: patricia.bassereau@curie.fr*
[b] *Department of Chemistry, Institute for Biophysical Dynamics, and James Franck Institute, The University of Chicago, Chicago, 60637 Illinois, USA*

the mechanical effect of Ca^{2+} ions on mixed PC/PS model membranes.

Results and discussion

A membrane at equilibrium will take a shape that corresponds to its spontaneous curvature. If a bilayer has homogeneously distributed lipids and equal composition in both layers, its spontaneous curvature is zero. Binding of particles may impose an asymmetry on the bilayer that leads to a nonzero spontaneous curvature.[19] We define positive curvature as when the membrane curves toward the binding leaflet, and negative otherwise (Fig. 1A).

Based on experimental and simulation evidence, monovalent cations insert between the lipids and dilate the membrane. Considering that, this way, lipids prefer to be further apart from one another, we expect this process to induce a positive spontaneous curvature (Fig. 1A, left). Conversely, as calcium contracts the lipid bilayer, it could lead to a negative spontaneous curvature where lipids in the calcium-binding leaflet are closer to one another (Fig. 1A, right).

To study this effect, we used a giant unilamellar vesicle (GUV) as a model membrane. By changing the pressure in the aspiration micropipette holding the GUV, we control its surface tension. We used a micron-sized bead, trapped with optical tweezers, to pull a tether from the GUV. Based on the movement of the bead, we track, in time, the retraction force of the tether. This force effectively represents the remodeling force of the membrane. Finally, with another pipette, we inject a Ca^{2+} solution in the vicinity of the system (Fig. 1B). We refer the reader to our previous work where we have shown that this method is very sensitive to detecting spontaneous curvature, evidenced by a sudden change in the tether-retraction force upon the injection of curvature-inducing molecules.[20,21]

An important advantage of injecting calcium solution directly onto the GUV and not pre-incubating the GUV is that we can compare the behavior in the absence and the presence of the ion on the same vesicle. Additionally, high bulk Ca^{2+} concentrations would induce undesirable fusion between vesicles. However, the concentration inside the pipette is not the same as the concentration in the vicinity of the membrane tether due to dilution. Therefore, we first determined how much of the injected solution is diluted. We injected a fluorescent marker linked to a membrane-binding protein and measured the fluorescence intensity from the exit of the injection pipette to the GUV (see Materials and methods). We found that the concentration of the injected solution is on average halved at the tether–GUV interface (Fig. 1C) and so, in the following calculations, we corrected the bulk calcium concentrations accordingly.

We carried out experiments on three different lipid compositions: (1) DOPC; (2) DOPC : DOPS (9 : 1); and (3) DOPC : DOPS (8 : 2). We did not test membranes with higher net charge, as the physiologically relevant concentration of PS lipids is in the 10–20% range.[22] Unexpectedly, the tether-retraction force did

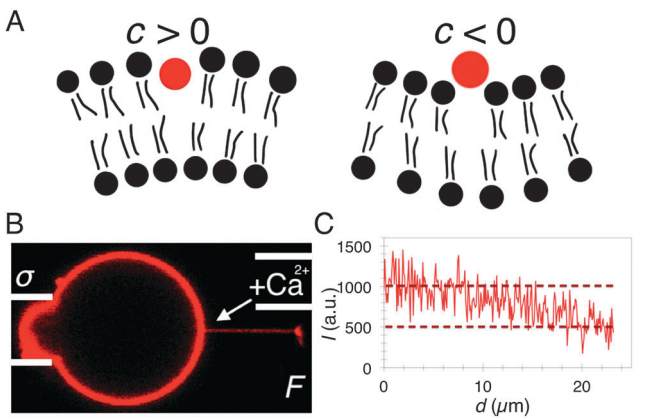

Fig. 1 (A) Scheme of a lipid bilayer with positive (left) and negative (right) spontaneous curvatures (c). Na^{+} dilates the lipid leaflet and is expected to induce a positive curvature, while Ca^{2+} compresses lipids and so it should induce a negative curvature. (B) Scheme of a tether-pulling experiment. An aspiration pipette controls membrane tension (σ), while the remodeling force (F) is measured from the displacement of the bead in the optical trap. We use another pipette to inject Ca^{2+}. (C) Dilution of the injected solution from the injection pipette exit to the base of the membrane tether, measured from fluorescence intensity of a labeled molecule. The plot shows one out of three measurements.

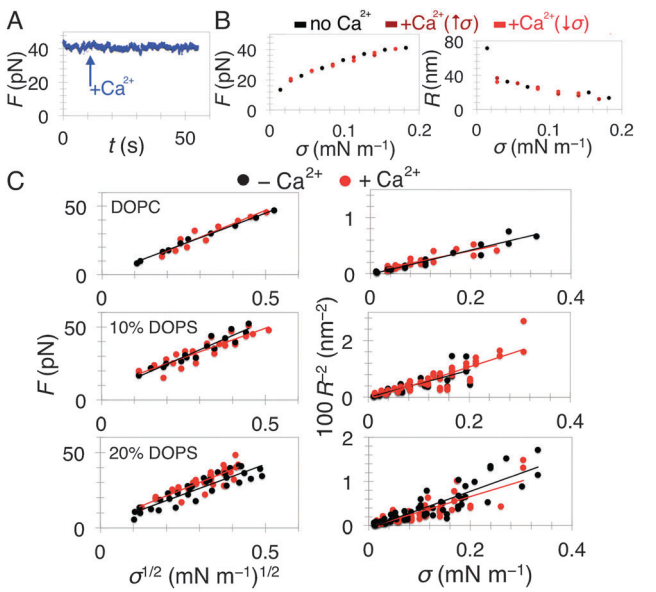

Fig. 2 Mechanics of DOPC and DOPC/DOPS membranes in the presence of NaCl and Ca^{2+}. (A) F as a function of time (t) during injection of 10 mM Ca^{2+} into a DOPC : DOPS = 8 : 2 GUV in 100 mM NaCl buffer. (B) F and R as a function of σ for a DOPC : DOPS = 8 : 2 GUV in 100 mM NaCl buffer (different examples from A). First, the measurement was done in the absence of Ca^{2+} (black dots) by stepwise increasing σ. Then, σ was reduced to a minimum and the measurement was repeated with 10 mM Ca^{2+} (maroon dots). Finally, continuing to inject, the measurement was repeated, but the tension was stepwise reduced (red dots). (C) Uncharged membrane displays no spontaneous curvature (top), while charged membranes show a weak negative spontaneous curvature (centre and bottom). The injection of 5, 10, or 50 mM Ca^{2+} does not have any detectable mechanical effect (due to the absence of the effect, we combine data points from all three Ca^{2+} concentrations for each composition). (top) 100% DOPC (N = 3), (centre) DOPC : DOPS = 9 : 1 (N = 3), and (bottom) DOPC : DOPS = 8 : 2 (N = 10). Refer to Table 1 for fitting parameters.

not deviate when injecting 10 mM Ca^{2+} on a 20% DOPS GUV (Fig. 2A). In addition, we could not observe a difference in the retraction force compared to a bare membrane at a wide range of surface tensions, up to 0.2 mN m^{-1} (Fig. 2B). To ensure that Ca^{2+} binding is not dependent on the direction of change in membrane tension, we confirmed that the forces superimpose whether there is stepwise increasing or decreasing tension (Fig. 2B, red and maroon dots). If binding of Ca^{2+} would induce a negative curvature, the bilayer would tend to curve away from the binding leaflet and thus oppose the positive curvature of the membrane tether. Hence, we would expect an increase in the tether-retraction force.

Moreover, a nonzero spontaneous curvature would affect the equilibrium radius of the pulled tether, compared to a reference membrane at the same membrane tension. We computed the radius of the tether from the measured lipid fluorescence intensity (see Materials and methods) and found no difference in the presence or absence of Ca^{2+} on 20% PS membranes (Fig. 2B).

Before discussing the implications of these results, we quantify the mechanical properties of the membrane. First, we derive the relationship between force, radius, and tension from the Helfrich Hamiltonian:[19]

$$H_t = \frac{\kappa}{2}\left(\frac{1}{r} - \frac{1}{R_0}\right)^2 A + \sigma A - fL \quad (1)$$

where H_t is the total free energy of the tether, κ is the membrane bending rigidity, r and R_0 are, respectively, the mean and spontaneous radii of curvature, A and L are, respectively, the area and the length of the tether, and f is the pulling force on the membrane. At equilibrium, r becomes the tether radius (R) and the force becomes the aforementioned tether-retraction force (F). To compute R and F, we minimize H_t with respect to L and R,[23] *i.e.* $\partial H_t/\partial R = 0$ and $\partial H_t/\partial L$, yielding,

$$F \approx 2\pi\sqrt{2\kappa\sigma} - 2\pi\kappa\frac{1}{R_0} \quad (2)$$

$$\frac{1}{R^2} = \frac{2\sigma}{\kappa} + \frac{1}{{R_0}^2} \quad (3)$$

The equations reveal that the tether curvature and the tether-retraction force scale as a square root of membrane tension. Fitting the model to our data gives κ and R_0. Considering that we measured the radius from the fluorescence intensity, we have two independent measurements of κ and R_0. We note that we cannot predict the direction of curvature from eqn (3) since R_0 appears as a square.

Just like the two GUVs presented in Fig. 2(A and B), we did not detect an appreciable difference in the radius or the force in the presence of up to 50 mM Ca^{2+} for any of the three membrane compositions, at a relatively wide range of membrane tensions, up to $\sim$0.3 mN m^{-1} (Fig. 2C).

Interestingly, even in the absence of Ca^{2+}, charged membranes displayed a low negative spontaneous curvature. Precisely, R_0, obtained from force measurements (eqn (2)) for reference 10% and 20% DOPS membranes, measured to be -120 nm and -200 nm, respectively (Table 1). We hypothesize two possible sources of the spontaneous curvature of charged membranes. First, the internal solution of vesicles is composed of pure sucrose, whereas the vesicles are immersed in a 100 mM NaCl buffer. Therefore, the repulsions of charged PS head groups are much less screened on the inner than on the outer leaflet. As a result, the membrane tends to curve inward to alleviate this effect, hence generating a negative curvature. Another possible contribution to the spontaneous curvature is the insertion of Na^+ into the bilayer. A shallow insertion (just below the phosphate, Fig. 1A) would induce a positive curvature, similar to the effect amphipathic protein helices have on the membrane.[24] Deeper penetration into the hydrocarbon core may, however, reverse the sign of curvature, as predicted by theory.[24] Considering that the effect is quite weak and is not affected by Ca^{2+}, we did not pursue its precise source.

It is still puzzling that Ca^{2+}, even at 50 mM does not impart any effect on 20% DOPS membranes. All experiments so far were performed in a 100 mM NaCl solution. If Na^+ indeed is inserted deeply into the bilayer, as predicted by the spontaneous curvature, it would be difficult to displace it with other ions.

We therefore repeated the experiment with 20% DOPS in the absence of NaCl. In this case, we observed a significant effect at 50 mM Ca^{2+} on both the retraction force and the tether radius. Surprisingly, however, both force and radius decreased compared to the reference membrane (Fig. 3). It appears that, contrary to our predictions based on the atomic structure, Ca^{2+} generates a positive membrane curvature, *i.e.* bends the bilayer toward the binding leaflet. Fitting eqn (2) to the data yields reverse and approximately twice the magnitude of the spontaneous curvature (R_0 = +110 nm) than the reference membrane in NaCl (Table 1).

It is generally assumed that the spontaneous curvature scales with the surface coverage of curvature-inducing particles.[25,26] We can write this expression as:

$$\frac{1}{R_0} = \frac{1}{\tilde{R}_0}x, \quad (4)$$

where $\tilde{R}_0$ is the effective spontaneous curvature (intrinsic to the binding particle) and x is the molar area fraction of bound Ca^{2+}. To calculate x, we use the Langmuir adsorption isotherm:

$$\frac{x}{1-x} = KC, \quad (5)$$

where C is the bulk ion concentration and K the equilibrium binding constant. Taking K = 650 M^{-1}, as previously measured on 20% DOPS membrane,[8] we obtain $x_{c=50\,mM}$ = 0.97. Therefore, $\tilde{R}_0$ for Ca^{2+} binding to 20% PS membranes is 107 nm, or 29 nm if calculated from fluorescence intensity (the corresponding effective spontaneous curvatures are 0.009 $\pm$ 0.009 nm^{-1} or 0.035 $\pm$ 0.0005 nm^{-1} if calculated from fluorescence intensity).

The lower concentration of Ca^{2+} (5 mM) induces five times lower, albeit still positive, curvature (R_0 = +540 nm). Compared to the size of the membrane, this value of spontaneous curvature is negligible and unlikely affects the morphology of the membrane. We list R_0 and κ from all experiments in Table 1.

Table 1 Fitting parameters obtained from all experiments (mean ± SD). Top values were obtained from force measurements using eqn (2), whereas parenthetic values were obtained from fluorescence measurements using eqn (3) and, in the case of the radius, have an ambiguous sign

	DOPC		10% DOPS		20% DOPS		20% DOPS, no NaCl	
	No Ca	+Ca^{2+}	No Ca	+Ca^{2+}	No Ca	+Ca^{2+}	+5 mM Ca^{2+}	+50 mM Ca^{2+}
$1/R_0$ (1/nm)	$1/3600 \pm 6 \times 10^{-5}$ $(1/100 \pm 1 \times 10^{-3})$	$1/350 \pm 2 \times 10^{-3}$ $(1/50 \pm 2 \times 10^{-3})$	$-1/120 \pm 4 \times 10^{-3}$ $(1/160 \pm 7 \times 10^{-4})$	$-1/60 \pm 8 \times 10^{-3}$ $(1/90 \pm 6 \times 10^{-4})$	$-1/200 \pm 5 \times 10^{-3}$ $(1/50 \pm 4 \times 10^{-4})$	$-1/160 \pm 6 \times 10^{-3}$ $(1/60 \pm 4 \times 10^{-4})$	$1/540 \pm 2 \times 10^{-3}$ $(1/50 \pm 9 \times 10^{-5})$	$1/110 \pm 9 \times 10^{-3}$ $(1/30 \pm 5 \times 10^{-4})$
κ (k_BT)	25.1 ± 1.4 (22.2 ± 1.5)	29.9 ± 7.0 (26.3 ± 3.4)	27.1 ± 5.1 (9.7 ± 0.7)	20.0 ± 3.9 (9.9 ± 1.2)	18.9 ± 3.4 (12.4 ± 1.1)	23.4 ± 4.5 (13.0 ± 1.2)	20.8 ± 1.9 (15.0 ± 0.5)	19.9 ± 2.9 (7.7 ± 0.7)

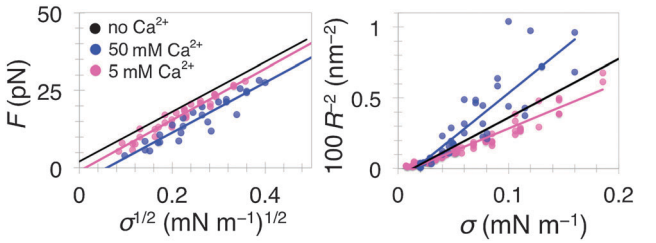

Fig. 3 Ca^{2+} induces a spontaneous curvature in the absence of NaCl. Fitting eqn (2) (left) and eqn (3) (right) to data obtained from DOPC : DOPS = 8 : 2 membrane in the presence of Ca^{2+} at 5 mM (N = 3) and 50 mM (N = 4). Refer to Table 1 for fitting parameters.

The observed positive spontaneous curvature is inconsistent with our initial predictions based on the lipid area contraction induced by Ca^{2+} and the proposed atomic coordination of Ca^{2+} with the phosphodiester group.[9,15,27,28] It seems that drawing an analogy with amphipathic protein helices, which insert below the phosphate, may be inaccurate. Instead, it is more likely that the strong repulsion between Ca^{2+} ions, brought by their high charge density, becomes even stronger upon lipid area contraction. The perturbation is alleviated by generating a positive curvature which will push Ca^{2+} ions apart.

Taken together, we learn that NaCl strongly screens any mechanical effect on the membrane, even at 50 mM Ca^{2+}. It has been reported that Na^+ competes with divalent cations for the binding on PS-containing membranes[8] and, even on 100% PS membranes, it can replace Ca^{2+} to a great extent.[29] To test the extent of electrostatic screening by NaCl, we performed ζ-potential measurements on small liposomes composed of 20% DOPS. We offset the concentration of salts with glucose to prevent the osmotic shock. In the absence of NaCl and Ca^{2+}, we found the potential to be −57.6 ± 2.4 mV (mean ± SD), however, it should be noted that in the absence of electrolytes, this measurement is uncertain. In the presence of NaCl, due to electrostatic screening, there is a decrease in magnitude with increased NaCl concentrations (Fig. 4), measuring −69.6 ± 3.6 mV (0.075 mM NaCl), −62.5 ± 2.1 mV (0.75 mM NaCl), −59.4 ± 1.9 mV (10 mM NaCl), and −52.4 ± 1.9 mV (20 mM NaCl), in good agreement with previously reported values.[8,30] In the absence of NaCl, the ζ-potential continuously increases

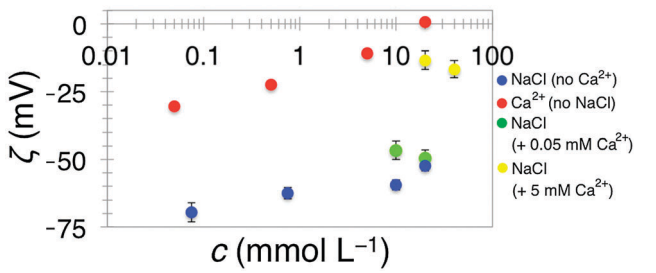

Fig. 4 ζ-Potential measurements of small liposomes (DOPC : DOPS = 8 : 2), as a function of salt concentration. Blue and red dots are measured in NaCl and Ca^{2+}, respectively. Green and yellow dots are measured in NaCl at a concentration indicated on the x-axis and it additionally contains, respectively, 0.05 or 5 mM Ca^{2+}.

with the concentration of Ca^{2+}, measuring -30.4 ± 0.9 mV (0.05 mM Ca^{2+}), -22.5 ± 1.4 mV (0.5 mM Ca^{2+}), -10.9 ± 0.5 mV (5 mM Ca^{2+}), and 0.7 ± 0.7 mV (20 mM Ca^{2+}) (Fig. 4).

Finally, we measured the ζ-potential in the presence of both ions. At 0.05 mM Ca^{2+}, we measured -46.6 ± 3.4 mV (10 mM NaCl) and -49.6 ± 3.2 mV (20 mM NaCl), whereas at 5 mM Ca^{2+} the values were -13.4 ± 0.8 mV (20 mM NaCl) and -16.7 ± 3.5 mV (40 mM NaCl) (Fig. 4). It therefore appears that NaCl screens Ca^{2+} relatively well at low concentrations (200–400 NaCl/Ca^{2+} molar ratio). At high Ca^{2+} concentrations (4–8 NaCl/Ca^{2+} molar ratio) the ζ-potential is also lower compared to NaCl-free conditions, however the screening effect is much weaker.

Conclusions

Our single-vesicle assay shows that Ca^{2+} ions induce a positive spontaneous curvature on negatively charged membranes. We propose that the repulsion between Ca^{2+} ions drives the membrane to curve outward, so as to minimize their interactions. We also speculate that if Ca^{2+} potentially drives the formation of PS domains, locally concentrating explicit charge would additionally result in a positive spontaneous curvature. Our simple model predicts that Ca^{2+} induces a positive radius of curvature on membranes with 20% net charge, with the magnitude of $\sim$110 nm. This magnitude of curvature scales linearly with the bound coverage of Ca^{2+}, which depends on the bulk concentration and the amount of charged lipids in the bilayer. We note that there is a quantitative discrepancy between the calculated spontaneous curvature from independent force and fluorescence measurements. Both of these measurements have limitations, especially at high tension, where the radius is very thin and the force is very high, so it is difficult to predict which measurement provides a more accurate estimate of the spontaneous curvature. Nevertheless, both measurements show qualitatively the same behavior in the presence and absence of NaCl, although fluorescence measurements systematically predict a lower radius of curvature.

What could be the consequences for a cell membrane? In cells, the concentration of Ca^{2+} is very tightly controlled. While extracellular solution contains $\sim$2.5 mM Ca^{2+}, the cytosolic concentration of Ca^{2+} is normally kept at only a nanomolar level. It seems unlikely that Ca^{2+} would induce a mechanical effect on a membrane of a quiescent cell. However, during various signaling events, its concentration may jump orders of magnitude and, combined with lipid clustering and area contraction, Ca^{2+} could sufficiently locally cover the membrane to induce budding and tubulation. Such consequences would be undesirable in signal transduction phenomena. Na^{+} ions completely inhibit the curvature effect of Ca^{2+}. Considering that our electrokinetic measurements revealed that Ca^{2+} still alters the electrostatic environment of the membrane, curvature screening is not a consequence of electrostatic screening. Instead, we propose that the tight binding and deep insertion of Na^{+} into the bilayer may serve as a very robust protection mechanism against nonspecific remodelling. Specialized proteins, such as those containing scaffolding domains, take the role of membrane sculptors, as they are specifically targeted to membrane remodeling sites.[31,32]

We hope our work will provide a better understanding of the extent the Ca^{2+} ions affect the membrane mechanical properties at relevant concentrations of charge in the membrane and in the presence of physiological ionic strength.

Materials and methods

Reagents

1,2-Dioleoyl-*sn-glycero*-3-phosphatidylcholine (DOPC), 1,2-dioleoyl-*sn-glycero*-3-phosphatidylserine (DOPS), and 1,2-distearoyl-*sn-glycero*-3-phosphoethanolamine-*N*-[biotinyl(polyethyleneglycol)-2000] (DSPE-PEG(2000)-biotin) were purchased from Avanti Polar Lipids. BODIPY-TR-C5-ceramide was purchased from Molecular Probes®. All reagents used to make buffers and β-casein from bovine milk (>99%) were purchased from Sigma-Aldrich.

Preparation of GUVs

GUVs were prepared by electroformation on indium tin oxide glass.[33] DOPC and DOPS were mixed at a desired molar ratio (see Results & discussion) to which we added 0.5% BODIPY-TR-C5-ceramide and 0.03% DSPE-PEG(2000)-biotin (both in molar percent). We smeared 10 μL of the mix (at 3 g L^{-1}) on each of the two slides of indium tin oxide glass, dried the film under vacuum for at least 1 h, then hydrated with sucrose. GUVs were grown under a sine voltage (1 V, 10 Hz) for approximately 1 h. The sucrose concentration was adjusted for each experiment so that the molalities of solutions inside and outside GUVs match.

Tether-pulling experiment

We followed the procedure described elsewhere.[20,21] The experimental chamber and the aspiration pipette ($\sim$5 μm in diameter at the tip) were immersed for 30 min in a solution of β-casein (5 g L^{-1}, dissolved in 100 mM NaCl and 10 mM HEPES) to minimize the adhesion of lipids to the glass surface. The chamber was then filled with the experimental solution (for experiments containing NaCl: 100 mM NaCl and 10 mM HEPES at pH = 7.4, and glucose to offset the molality inside GUVs; for saltless experiments: glucose with equal molality as the sucrose inside GUVs). Another pipette was filled with 10, 20, or 100 mM $CaCl_2$ (see text) and if necessary was offset with glucose to match the molality of the experimental solution. The chamber was sealed with oil after $\sim$10 min to prevent evaporation. GUVs with enough excess area to form an aspiration tongue[34,35] were aspirated in a micropipette. Membrane tension was controlled *via* the aspiration pressure, calculated using the Laplace relation: $\sigma = 0.5\Delta p r_p/(1 - r_p/r_v)$, where Δp is the hydrostatic pressure, and r_p and r_v are radii of the pipette and the vesicle, respectively.[34] A tether was created by bringing the GUV in contact with a streptavidin-coated polystyrene bead, $\sim$3 μm in diameter (Spherotec), trapped with optical tweezers. We measured the tether-retraction force as $F = k(a - a_0)$, where a is the actual and a_0 the equilibrium position of the bead, tracked

using a bright field microscope and k is the stiffness of the trap, calibrated using the viscous drag method.[36] A typical measurement was performed by stepwise increasing the aspiration pressure and measuring the force and fluorescence for several minutes at each pressure. The measurement was then repeated by approaching the injection pipette and injecting Ca^{2+}, by either starting over from low pressure or reducing stepwise from high pressure. The direction of pressure did not affect the results (see text). In experiments with no NaCl, we could only measure the steps after injecting Ca^{2+}, as the streptavidin–biotin interactions require the presence of ions. We conducted experiments by injecting 100 mM Ca^{2+} (using the pipette, see above for the dilution factor) and incubating the vesicles with 5 mM Ca^{2+}. We measured the radius of the tether using the following relationship: $R = C_f I_t/I_v$, where I_t and I_v are the lipid fluorescence intensities of the tether and the vesicle, respectively, and C_f = 200 ± 50 is the calibration factor deduced previously.[20]

We determined the dilution of the injected solution by injecting ~2 μM Alexa488 from a similar distance and at an injection pressure (10–20 Pa) as in all experiments with calcium. Alexa488 was bound to a membrane-binding protein, β2 centaurin, kindly provided by Harvey McMahon. We then measured the decrease in fluorescence intensity as a function of the distance from the pipette (three measurements). It should be kept in mind that assuming the same dilution factor for Ca^{2+} as the marker likely overestimates the near-vesicle concentration, considering that Ca^{2+} has a lower hydrodynamic radius and it would diffuse out faster than the fluorescent marker. Taking the upper-limiting case ensures we do not overestimate the effect we quantify.

Preparation of small liposomes

The lipid mix composed of DOPC : DOPS (4 : 1, molar ratios) was dried under nitrogen to obtain 1 mg of the dry mass. The mix was hydrated in 1 mL of sucrose then freeze–thawed five times, followed by extrusion through a polycarbonate filter with pores 100 nm in diameter. We confirmed the final size of liposomes to be 106 ± 7 nm (N = 4) with dynamic light scattering.

ζ-Potential measurements

We used a Malvern Zetasizer Nano ZS (Malvern Instruments Ltd) to measure the electrophoretic mobility, which was converted to the ζ-potential using Henry's equation $\zeta = 3u\eta/(2\varepsilon f)$,[37] where u is the electrophoretic mobility, η the viscosity of the solution, ε the dielectric constant, and f Henry's function, calculated using:[38] $f = 1 + 0.5[1 + (2.5/\lambda a[1 + 2e^{-\lambda a}])]$, where a = 100 nm was taken as the particle radius of curvature and λ is the inverse Debye length, calculated using: $\lambda = \sqrt{\sum_{i=1}^{N} e^2 z_i^2 n_i \Big/ \varepsilon_r \varepsilon_0 k_B T}$. N is the number of ionic species, e is the elementary charge, z_i and n_i are the charge number and the amount of ion i, respectively, ε_r and ε_0 are the relative and vacuum electric permittivity, respectively, k_B is the Boltzmann constant, and T is the thermodynamic temperature.[37] In the case of pure glucose, f = 1.0 was approximated. All measurements were taken three times.

Acknowledgements

We acknowledge the support from the Chateaubriand Fellowship (MS) and the France and Chicago Collaborating in The Sciences fund (MS). The Bassereau team is a member of the LabEx CelTisPhyBio (ANR-11-LABX0038), Paris Sciences et Lettres (ANR-10-IDEX-0001-02) and the French research consortium CellTiss. We thank Coline Prévost, Tom Rapoport and Misha Kozlov for insightful discussions.

References

1 D. E. Clapham, *Cell*, 2007, **131**, 1047–1058.
2 M. E. Monteiro, M. J. Sarmento and F. Fernandes, *Biochem. Soc. Trans.*, 2014, **42**, 1441–1446.
3 O. H. Petersen, M. Michalak and A. Verkhratsky, *Cell Calcium*, 2005, **38**, 161–169.
4 P. K. Tarafdar, H. Chakraborty, S. M. Dennison and B. R. Lentz, *Biophys. J.*, 2012, **103**, 1880–1889.
5 R. Ekerdt and D. Papahadjopoulos, *Proc. Natl. Acad. Sci. U. S. A.*, 1982, **79**, 2273–2277.
6 T. Ito and S. I. Ohnishi, *Biochim. Biophys. Acta*, 1974, **352**, 29–37.
7 D. Papahadjopoulos, S. Nir and N. Duzgunes, *J. Bioenerg. Biomembr.*, 1990, **22**, 157–179.
8 C. G. Sinn, M. Antonietti and R. Dimova, *Colloids Surf., A*, 2006, **282**, 410–419.
9 P. T. Vernier, M. J. Ziegler and R. Dimova, *Langmuir*, 2009, **25**, 1020–1027.
10 I. Levental, A. Cebers and P. A. Janmey, *J. Am. Chem. Soc.*, 2008, **130**, 9025–9030.
11 M. Sovago, G. W. Wurpel, M. Smits, M. Muller and M. Bonn, *J. Am. Chem. Soc.*, 2007, **129**, 11079–11084.
12 R. A. Bockmann, A. Hac, T. Heimburg and H. Grubmuller, *Biophys. J.*, 2003, **85**, 1647–1655.
13 P. Mukhopadhyay, L. Monticelli and D. P. Tieleman, *Biophys. J.*, 2004, **86**, 1601–1609.
14 S. A. Pandit and M. L. Berkowitz, *Biophys. J.*, 2002, **82**, 1818–1827.
15 U. R. Pedersen, C. Leidy, P. Westh and G. H. Peters, *Biochim. Biophys. Acta*, 2006, **1758**, 573–582.
16 Y. H. Wang, A. Collins, L. Guo, K. B. Smith-Dupont, F. Gai, T. Svitkina and P. A. Janmey, *J. Am. Chem. Soc.*, 2012, **134**, 3387–3395.
17 H. Binder and O. Zschornig, *Chem. Phys. Lipids*, 2002, **115**, 39–61.
18 G. van Meer, D. R. Voelker and G. W. Feigenson, *Nat. Rev. Mol. Cell Biol.*, 2008, **9**, 112–124.
19 W. Helfrich, *Z. Naturforsch., C: J. Biosci.*, 1973, **28**, 693–703.
20 B. Sorre, A. Callan-Jones, J. Manzi, B. Goud, J. Prost, P. Bassereau and A. Roux, *Proc. Natl. Acad. Sci. U. S. A.*, 2012, **109**, 173–178.

21 H. F. Renard, M. Simunovic, J. Lemiere, E. Boucrot, M. D. Garcia-Castillo, S. Arumugam, V. Chambon, C. Lamaze, C. Wunder, A. K. Kenworthy, A. A. Schmidt, H. T. McMahon, C. Sykes, P. Bassereau and L. Johannes, *Nature*, 2015, **517**, 493–496.
22 K. Boesze-Battaglia and R. Schimmel, *J. Exp. Biol.*, 1997, **200**, 2927–2936.
23 I. Derenyi, F. Julicher and J. Prost, *Phys. Rev. Lett.*, 2002, **88**, 238101.
24 A. Zemel, A. Ben-Shaul and S. May, *J. Phys. Chem. B*, 2008, **112**, 6988–6996.
25 S. Leibler, *J. Phys.*, 1986, **47**, 507–516.
26 R. Lipowsky, *Faraday Discuss.*, 2013, **161**, 305–331; discussion 419–359.
27 J. M. Boettcher, R. L. Davis-Harrison, M. C. Clay, A. J. Nieuwkoop, Y. Z. Ohkubo, E. Tajkhorshid, J. H. Morrissey and C. M. Rienstra, *Biochemistry*, 2011, **50**, 2264–2273.
28 J. Seelig, *Cell Biol. Int. Rep.*, 1990, **14**, 353–360.
29 R. Kurland, C. Newton, S. Nir and D. Papahadjopoulos, *Biochim. Biophys. Acta*, 1979, **551**, 137–147.
30 F. J. Carrion, A. Delamaza and J. L. Parra, *J. Colloid Interface Sci.*, 1994, **164**, 78–87.
31 H. T. McMahon and J. L. Gallop, *Nature*, 2005, **438**, 590–596.
32 M. Simunovic and P. Bassereau, *Biol. Chem.*, 2014, **395**, 275–283.
33 M. I. Angelova, S. Soléau, P. Méléard, F. Faucon and P. Bothorel, in *Trends in Colloid and Interface Science VI*, ed. C. Helm, M. Lösche and H. Möhwald, Steinkopff, 1992, vol. 89, pp. 127–131.
34 R. Kwok and E. Evans, *Biophys. J.*, 1981, **35**, 637–652.
35 D. Cuvelier, I. Derenyi, P. Bassereau and P. Nassoy, *Biophys. J.*, 2005, **88**, 2714–2726.
36 K. C. Neuman and S. M. Block, *Rev. Sci. Instrum.*, 2004, **75**, 2787–2809.
37 A. V. Delgado, F. Gonzalez-Caballero, R. J. Hunter, L. K. Koopal and J. Lyklema, *J. Colloid Interface Sci.*, 2007, **309**, 194–224.
38 H. Ohshima, *J. Colloid Interface Sci.*, 1994, **164**, 510–513.

